Nikolaos Georgakarakos
New York University Abu Dhabi, UAE

Orbital Stability of Circumbinary Systems

The formation and long-term evolution of circumbinary planetary systems across the H-R diagram

Florence, 15/01/2025

5788 exoplanets

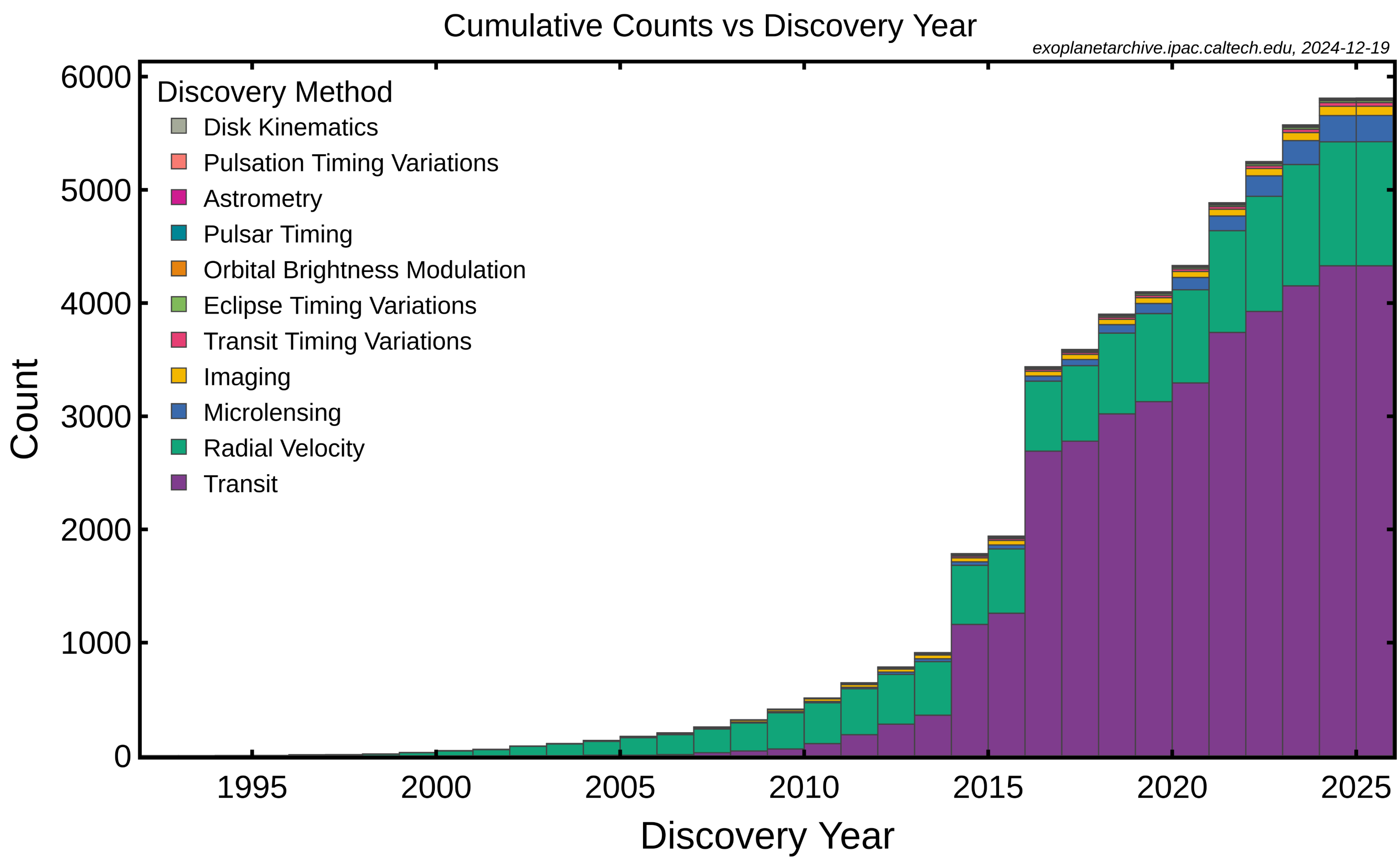

Credit: NASA Exoplanet Archive

More than 220 planets in binary systems

NASA EXOPLANET ARCHIVE

NASA EXOPLANET SCIENCE INSTITUTE

Home | About Us | Data | Tools | Support

Select Columns | Download Table | Plot Table | View Documentation | User Pref

Planetary Systems

Planet Name	Host Name	Number of Stars	Number of Planets
		2	
11 Com b	11 Com	2	1
11 Com b	11 Com	2	1
11 Com b	11 Com	2	1
18 Del b	18 Del	2	1
18 Del b	18 Del	2	1
18 Del b	18 Del	2	1
2MASS J01033563-5515561 AB b	2MASS J0103356	2	1
2MASS J0249-0557 c	2MASS J0249-05!	2	1
42 Dra b	42 Dra	2	1
CoRoT-2 b	CoRoT-2	2	1
CoRoT-2 b	CoRoT-2	2	1
CoRoT-2 b	CoRoT-2	2	1
CoRoT-2 b	CoRoT-2	2	1
CoRoT-2 b	CoRoT-2	2	1
CoRoT-2 b	CoRoT-2	2	1
CoRoT-2 b	CoRoT-2	2	1
CoRoT-2 b	CoRoT-2	2	1

Circumstellar configuration

(or S-type)

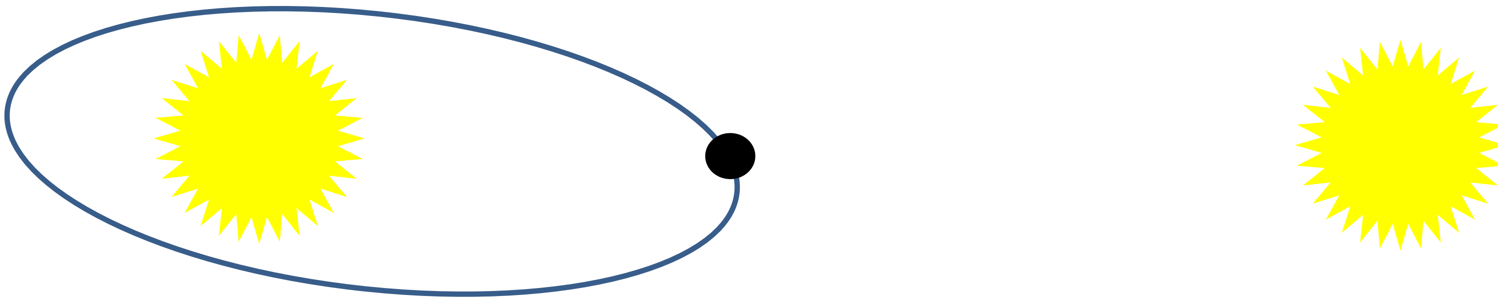

Circumbinary configuration

(or P-type)

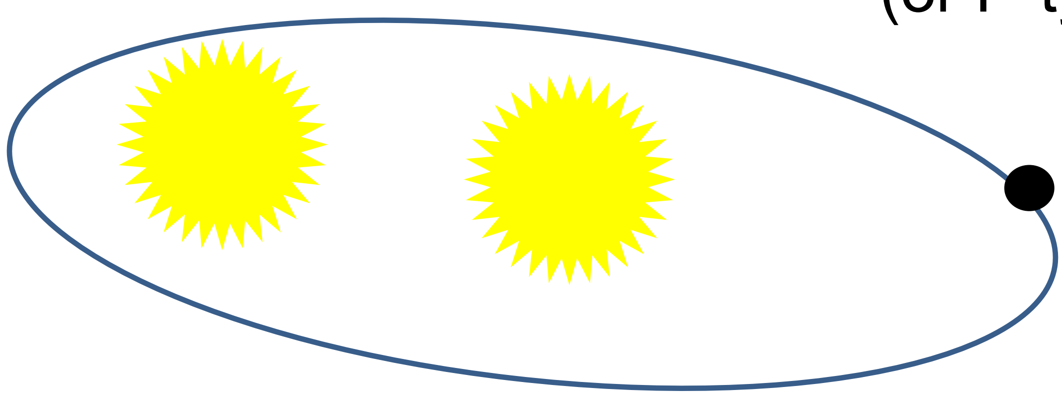

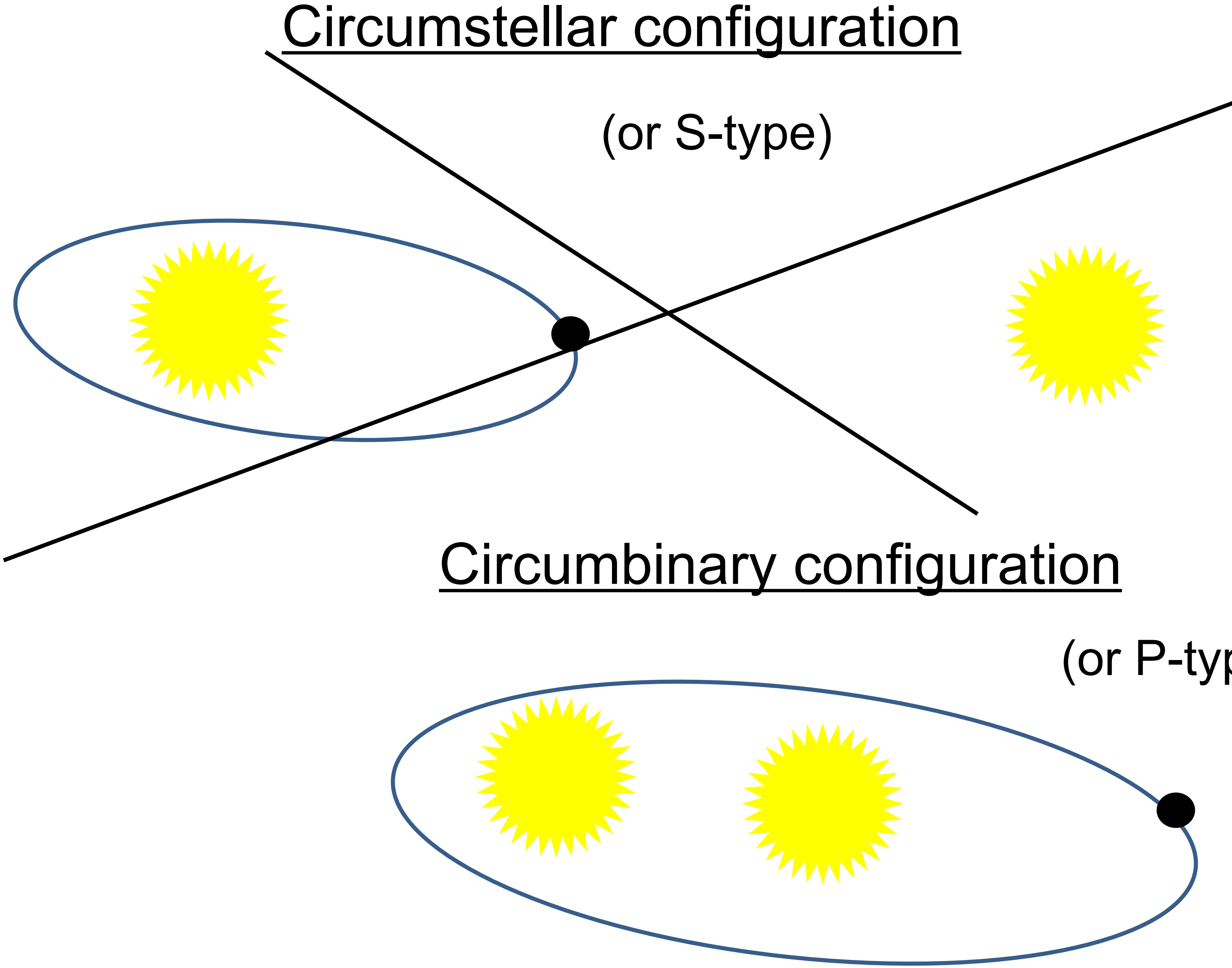
Circumstellar configuration
(or S-type)
Circumbinary configuration
(or P-type)

Circumbinary planets

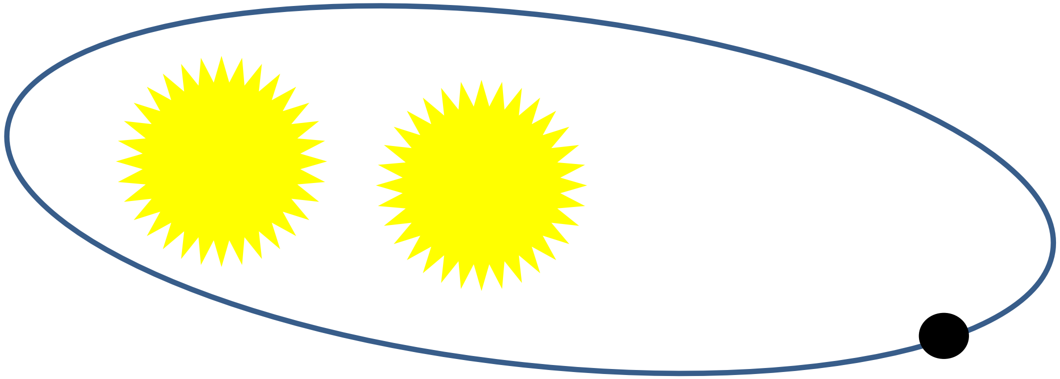

We want to find out where a planet is allowed to be around the binary without its orbit being destabilized

Important for many processes:

planet formation
planet detection
habitability etc.

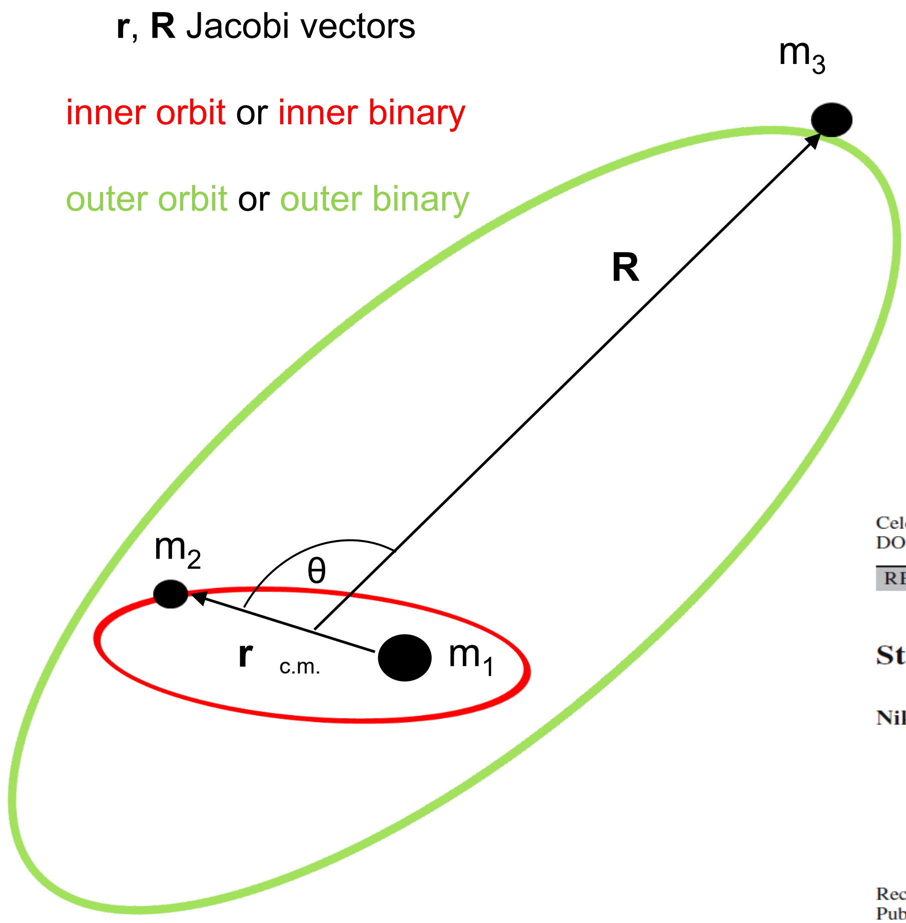

Celestial Mech Dyn Astr (2008) 100:151–168
DOI 10.1007/s10569-007-9109-2

REVIEW ARTICLE

Stability criteria for hierarchical triple systems

Nikolaos Georgakarakos

Received: 7 March 2007 / Revised: 3 September 2007 / Accepted: 28 November 2007 /
Published online: 3 January 2008

Abstract In this paper, we give a summary of stability criteria that have been derived for hierarchical triple systems over the past few decades. We give a brief description and we discuss the criteria that are based on the generalisation of the concept of zero velocity surfaces of the restricted three body problem, to the general case. We also present criteria that have to do with escape of one of the bodies. Then, we talk about the criteria that have been derived using data from numerical integrations. Finally, we report on criteria that involve the concept of chaos. In all cases, wherever possible, we discuss advantages and disadvantages of the criteria and the methods their derivation was based on, and some comparison is made in several cases.

Keywords Celestial mechanics · Three body problem · Stability

Some historical background

THE ASTRONOMICAL JOURNAL VOLUME 82, NUMBER 9 SEPTEMBER 1977

Planetary orbits in binary stars

Robert S. Harrington
U.S. Naval Observatory, Washington, DC 20390
(Received 19 May 1977; revised 24 June 1977)

Numerical integrations of the general three-body problem, with one component having a planetary mass, indicate that stable planetary orbits can exist in binary stars. The limitation for stability is that the ratio of the periastron distance of the outer tertiary component to the semimajor axis of the close component be somewhere in the range 3–4, regardless of which of the components is the planet. For most known binaries, this region of stability includes the region of habitability for planets.

Harrington (1977)

Numerical simulations of HTS:

- 2 stars + planet (both S-type & P-type)
- Planar systems
- Largest mass ratio not exceeding 100:1
- Planet mass $m_p = M_E, M_J$
- Binary eccentricity e_b=0, 0.5
- Planetary eccentricity e_p=0
- Time of integrations: 10-20 outer revolutions
- Stability : semi-major axes and eccentricities showed no large changes

THE ASTRONOMICAL JOURNAL VOLUME 82, NUMBER 9 SEPTEMBER 1977

Planetary orbits in binary stars

Robert S. Harrington
U.S. Naval Observatory, Washington, DC 20390
(Received 19 May 1977; revised 24 June 1977)

Numerical integrations of the general three-body problem, with one component having a planetary mass, indicate that stable planetary orbits can exist in binary stars. The limitation for stability is that the ratio of the periastron distance of the outer tertiary component to the semimajor axis of the close component be somewhere in the range 3–4, regardless of which of the components is the planet. For most known binaries, this region of stability includes the region of habitability for planets.

Harrington (1977)

Numerical simulations of HTS:

- 2 stars + planet (both S-type & P-type)
- Planar systems
- Largest mass ratio not exceeding 100:1
- Planet mass $m_p = M_E, M_J$
- Binary eccentricity e_b=0, 0.5
- Planetary eccentricity e_p=0
- Time of integrations: 10-20 outer revolutions
- Stability : semi-major axes and eccentricities showed no large changes

$$q_2/a_1 \geq F \equiv A\left\{1 + B\log\left[\frac{1 + m_3/(m_1+m_2)}{3/2}\right]\right\} + K$$

I	*A*	*B*
0	3.50	0.70
II	2.75	0.64

q_2 outer pericenter distance
a_1 inner pair semi-major axis

K=0 mean fit
K=2 upper limit

Astron. Astrophys. 167, 379–386 (1986)

ASTRONOMY AND ASTROPHYSICS

Critical orbits in the elliptic restricted three-body problem

R. Dvorak
Institut für Astronomie, Universität Wien, Türkenschanzstrasse 17, A-1180 Wien, Austria

Received March 14, accepted June 12, 1986

Dvorak (1986)

Numerical simulations of HTS:

- 2 stars + planet (P-type)
- Planar systems
- Equal mass binary
- Planet = massless
- Binary eccentricity e_b=0-0.9
- Planetary eccentricity e_p=0
- Time of integrations: 500 binary periods
- Stability : eccentricitiy < 0.3

Astron. Astrophys. 167, 379–386 (1986)

ASTRONOMY AND ASTROPHYSICS

Critical orbits in the elliptic restricted three-body problem

R. Dvorak
Institut für Astronomie, Universität Wien, Türkenschanzstrasse 17, A-1180 Wien, Austria

Received March 14, accepted June 12, 1986

Dvorak (1986)

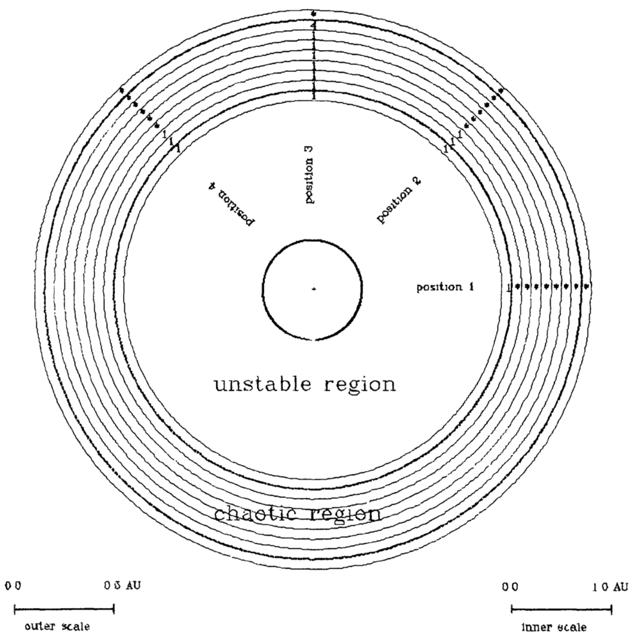

Numerical simulations of HTS:

- 2 stars + planet (P-type)
- Planar systems
- Equal mass binary
- Planet = massless
- Binary eccentricity e_b=0-0.9
- Planetary eccentricity e_p=0
- Time of integrations: 500 binary periods
- Stability : eccentricity < 0.3

$$\mathrm{UCO} = 2.37 + 2.76\, e - 1.04\, e^2$$

and

$$\mathrm{LCO} = 2.09 + 2.79\, e - 2.07\, e^2$$

UCO : **U**pper **C**ritical **O**rbit
LCO : **L**ower **C**ritical **O**rbit

- That work was extended to unequal mass binaries by Dvorak et al. (1989) and to retrograde orbits by Hong & van Putten (2021)

- Rabl & Dvorak (1988) provided stability limits for S-type orbits.

THE ASTRONOMICAL JOURNAL, 117:621–628, 1999 January

LONG-TERM STABILITY OF PLANETS IN BINARY SYSTEMS

MATTHEW J. HOLMAN
Harvard-Smithsonian Center for Astrophysics, 60 Garden Street, Cambridge, MA 02138
AND
PAUL A. WIEGERT
Department of Physics and Astronomy, York University, Toronto, Ontario M3J 3P1, Canada
Received 1998 July 31 ; accepted 1998 September 23

Holman & Wiegert 1999

INITIAL CONDITIONS FOR THE BINARIES AND TEST PARTICLES

Inner Region	Outer Region
Binaries	
$a_b = 1.0$	
$0.1 \leq \mu \leq 0.9$	$0.1 \leq \mu \leq 0.5$
$\Delta\mu = 0.1$	
$0.0 \leq e \leq 0.8$	$0.0 \leq e \leq 0.7$
$\Delta e = 0.1$	
Binary phase: periapse or apapse	
Test Particles	
$0.02a_b \leq a \leq 0.5a_b$	$1.0a_b \leq a \leq 5.0a_b$
$\Delta a = 0.0025$–$0.01a_b$	$\Delta a = 0.1a_b$
$e_p = i = \Omega = \omega = 0.0$	
$M = 0°, 45°, 90°, 135°, 180°, 225°, 270°, 315°$	

NOTE.—The binary semimajor axis is a_b, its eccentricity is e, and its mass ratio $\mu = m_2/(m_1 + m_2)$. A test particle's initial semimajor axis, eccentricity, inclination relative to the binary plane, longitude of the ascending node, argument of perihelion, and mean anomaly are designated by $a, e_p, i, \Omega, \omega$, and M, respectively.

Numerical simulations of HTS:

- 2 stars + planet (S-type & P-type)
- Planar systems
- Planet = massless
- Planetary eccentricity e_p=0
- Time of integrations: 10^4 binary periods
- Stability : escape or close encounter with the stars

'At the end of the integrations, the semimajor axis at which the test particles at all initial longitudes survived the full integration time is determined. We call this the critical semimajor axis.'

THE ASTRONOMICAL JOURNAL, 117:621–628, 1999 January

LONG-TERM STABILITY OF PLANETS IN BINARY SYSTEMS

MATTHEW J. HOLMAN
Harvard-Smithsonian Center for Astrophysics, 60 Garden Street, Cambridge, MA 02138
AND
PAUL A. WIEGERT
Department of Physics and Astronomy, York University, Toronto, Ontario M3J 3P1, Canada
Received 1998 July 31 ; accepted 1998 September 23

Holman & Wiegert 1999

INITIAL CONDITIONS FOR THE BINARIES AND TEST PARTICLES

Inner Region	Outer Region
Binaries	
$a_b = 1.0$	
$0.1 \le \mu \le 0.9$	$0.1 \le \mu \le 0.5$
$\Delta\mu = 0.1$	
$0.0 \le e \le 0.8$	$0.0 \le e \le 0.7$
$\Delta e = 0.1$	
Binary phase: periapse or apapse	
Test Particles	
$0.02a_b \le a \le 0.5a_b$	$1.0a_b \le a \le 5.0a_b$
$\Delta a = 0.0025$–$0.01a_b$	$\Delta a = 0.1a_b$
$e_p = i = \Omega = \omega = 0.0$	
$M = 0°, 45°, 90°, 135°, 180°, 225°, 270°, 315°$	

NOTE.—The binary semimajor axis is a_b, its eccentricity is e, and its mass ratio $\mu = m_2/(m_1 + m_2)$. A test particle's initial semimajor axis, eccentricity, inclination relative to the binary plane, longitude of the ascending node, argument of perihelion, and mean anomaly are designated by $a, e_p, i, \Omega, \omega$, and M, respectively.

Numerical simulations of HTS:

- 2 stars + planet (S-type & P-type)
- Planar systems
- Planet = massless
- Planetary eccentricity e_p=0
- Time of integrations: 10^4 binary periods
- Stability : escape or close encounter with the stars

'At the end of the integrations, the semimajor axis at which the test particles at all initial longitudes survived the full integration time is determined. We call this the critical semimajor axis.'

S-type

$$a_c = [(0.464 \pm 0.006) + (-0.380 \pm 0.010)\mu + (-0.631 \pm 0.034)e + (0.586 \pm 0.061)\mu e + (0.150 \pm 0.041)e^2 + (-0.198 \pm 0.074)\mu e^2]a_b$$

P-type

$$a_c = (1.60 \pm 0.04) + (5.10 \pm 0.05)e + (-2.22 \pm 0.11)e^2 + (4.12 \pm 0.09)\mu + (-4.27 \pm 0.17)e\mu + (-5.09 \pm 0.11)\mu^2 + (4.61 \pm 0.36)e^2\mu^2 .$$

Holman & Wiegert 1999

P-type

Quarles et al. (2018):

- Extended binary mass ratio

S-type

Quarles et al. (2020):

- 3D orbits

Same function as H&W but with adjusted coefficients.

Holman & Wiegert 1999

Comment: In many cases for P-type systems, ”islands” of instability were noticed at values greater than the critical semimajor axis. This was due to the definition of the critical semimajor axis in H&W.

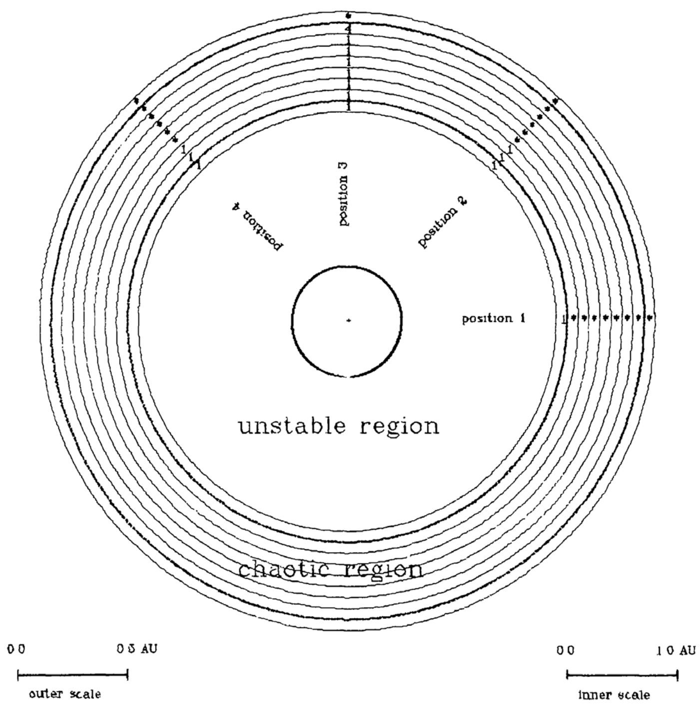

Kepler-16b (Chavez et al. 2015)

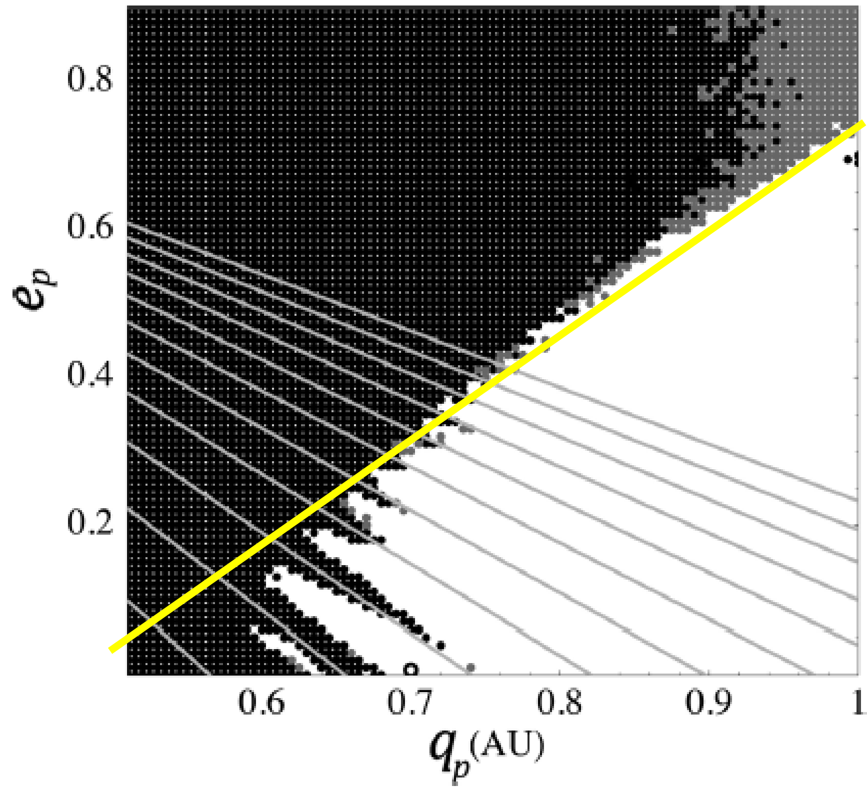

Mon. Not. R. Astron. Soc. 321, 398–420 (2001)

Tidal interactions in star cluster simulations

Rosemary A. Mardling[1★] and Sverre J. Aarseth[2]
[1]Mathematics Department, Monash University, Clayton 3800, Victoria, Australia
[2]Institute of Astronomy, University of Cambridge, Cambridge

Mardling & Aarseth (1999,2001)

Accepted 2000 August 23. Received 2000 May 26; in original form 1999 April 23

Similarities between escape in HTS and chaotic energy exchange in the binary – tides problem.

$$R_p^{crit} = 2.8 a_b \left[\left(1 + \frac{m_3}{m_1 + m_2}\right) \frac{1 + e_{out}}{(1 - e_{out})^{\frac{1}{2}}} \right]^{\frac{2}{5}} \left(1 - 0.3 \frac{I_m}{180}\right)$$

R_p^{crit} is the critical outer pericenter distance and I_m is the mutual inclination.

If $R_p^{crit} \leq R_p^{out}$ then the system is stable.

The above equation was not tested for planetary mass bodies.

A&A, 680, A29 (2023)
https://doi.org/10.1051/0004-6361/202244329

Astronomy & Astrophysics

Stability of coorbital planets around binaries

Stefan Adelbert[1], Anna B. T. Penzlin[1,2], Christoph M. Schäfer[1], Wilhelm Kley[1,⋆], Billy Quarles[3], and Rafael Sfair[1,4]

[1] Institut für Astronomie und Astrophysik, Universität Tübingen, Auf der Morgenstelle 10, 72076 Tübingen, Germany
e-mail: stefan.adelbert@uni-tuebingen.de
[2] Astrophysics Group, Department of Physics, Imperial College London, Prince Consort Rd, London, SW7 2AZ, UK
e-mail: a.penzlin@imperial.ac.uk
[3] Department of Applied Mathematics and Physics, Valdosta State University, Valdosta GA, 31698, USA
[4] Grupo de Dinâmica Orbital e Planetologia, São Paulo State University, UNESP, Guaratinguetá, CEP 12516-410, São Paulo, Brazil

Received 23 June 2022 / Accepted 10 October 2023

ABSTRACT

In previous hydrodynamical simulations, we found a mechanism for nearly circular binary stars, such as Kepler-413, to trap two planets in a stable 1:1 resonance. Therefore, the stability of coorbital configurations becomes a relevant question for planet formation around binary stars. For this work, we investigated the coorbital planet stability using a Kepler-413 analogue as an example and then expanded the parameters to study a general n-body stability of planet pairs in eccentric horseshoe orbits around binaries. The stability was tested by evolving the planet orbits for 10^5 binary periods with varying initial semi-major axes and planet eccentricities. The unstable region of a single circumbinary planet is used as a comparison to the investigated coorbital configurations in this work. We confirm previous findings on the stability of single planets and find a first order linear relation between the orbit eccentricity e_p and pericentre to identify stable orbits for various binary configurations. Such a linear relation is also found for the stability of 1:1 resonant planets around binaries. Stable orbits for eccentric horseshoe configurations exist with a pericentre closer than seven binary separations and, in the case of Kepler-413, the pericentre of the first stable orbit can be approximated by $r_{c,peri} = (2.90\, e_p + 2.46)\, a_{bin}$.

Key words. binaries: general – planets and satellites: dynamical evolution and stability

<u>Adelbert et al. 2023</u>

<u>Numerical simulations of HTS</u>:

- 2 stars + planet (P-type)
- Coplanar systems
- Same binary mass ratio as H&W
- Planet mass $m_p = 10^{-4} M_b$?
- Binary eccentricity e_b=0-0.5
- Planetary eccentricity e_p=0-0.9
- Time of integrations: 10^5 binary periods
- Stability : planetary semi-major axis < 20% change of its initial value

A&A, 680, A29 (2023)
https://doi.org/10.1051/0004-6361/202244329

Astronomy & Astrophysics

Stability of coorbital planets around binaries

Stefan Adelbert[1], Anna B. T. Penzlin[1,2], Christoph M. Schäfer[1], Wilhelm Kley[1,⋆], Billy Quarles[3], and Rafael Sfair[1,4]

[1] Institut für Astronomie und Astrophysik, Universität Tübingen, Auf der Morgenstelle 10, 72076 Tübingen, Germany
e-mail: stefan.adelbert@uni-tuebingen.de
[2] Astrophysics Group, Department of Physics, Imperial College London, Prince Consort Rd, London, SW7 2AZ, UK
e-mail: a.penzlin@imperial.ac.uk
[3] Department of Applied Mathematics and Physics, Valdosta State University, Valdosta GA, 31698, USA
[4] Grupo de Dinâmica Orbital e Planetologia, São Paulo State University, UNESP, Guaratinguetá, CEP 12516-410, São Paulo, Brazil

Received 23 June 2022 / Accepted 10 October 2023

ABSTRACT

In previous hydrodynamical simulations, we found a mechanism for nearly circular binary stars, such as Kepler-413, to trap two planets in a stable 1:1 resonance. Therefore, the stability of coorbital configurations becomes a relevant question for planet formation around binary stars. For this work, we investigated the coorbital planet stability using a Kepler-413 analogue as an example and then expanded the parameters to study a general n-body stability of planet pairs in eccentric horseshoe orbits around binaries. The stability was tested by evolving the planet orbits for 10^5 binary periods with varying initial semi-major axes and planet eccentricities. The unstable region of a single circumbinary planet is used as a comparison to the investigated coorbital configurations in this work. We confirm previous findings on the stability of single planets and find a first order linear relation between the orbit eccentricity e_p and pericentre to identify stable orbits for various binary configurations. Such a linear relation is also found for the stability of 1:1 resonant planets around binaries. Stable orbits for eccentric horseshoe configurations exist with a pericentre closer than seven binary separations and, in the case of Kepler-413, the pericentre of the first stable orbit can be approximated by $r_{c,peri} = (2.90\, e_p + 2.46)\, a_{bin}$.

Key words. binaries: general – planets and satellites: dynamical evolution and stability

Adelbert et al. 2023

Numerical simulations of HTS:

- 2 stars + planet (P-type)
- Coplanar systems
- Same binary mass ratio as H&W
- Planet mass $m_p = 10^{-4} M_b$?
- Binary eccentricity e_b=0-0.5
- Planetary eccentricity e_p=0-0.9
- Time of integrations: 10^5 binary periods
- Stability : planetary semi-major axis > 20% change of its initial value

$$
\begin{aligned}
r_{c,peri}/a_{bin} = {} & (1.36 \pm 0.05) \\
& + (5.79 \pm 0.19)e_{bin} - (5.87 \pm 0.39)e_{bin}^2 \\
& + (1.99 \pm 0.32)\mu_{bin} - (3.14 \pm 0.52)\mu_{bin}^2 \\
& + [(1.85 \pm 0.05) \\
& - (2.10 \pm 0.46)e_{bin}^2 + (3.00 \pm 0.52)e_{bin}\mu_{bin}]e_p .
\end{aligned}
$$

THE ASTRONOMICAL JOURNAL, 168:224 (16pp), 2024 November https://doi.org/10.3847/1538-3881/ad7a78

Empirical Stability Criteria for 3D Hierarchical Triple Systems. I. Circumbinary Planets

Nikolaos Georgakarakos[1,2], Siegfried Eggl[3], Mohamad Ali-Dib[2], and Ian Dobbs-Dixon[1,2]
[1] Division of Science, New York University Abu Dhabi, PO Box 129188, Abu Dhabi, UAE; ng53@nyu.edu
[2] Center for Astrophysics and Space Science (CASS), New York University Abu Dhabi, PO Box 129188, Abu Dhabi, UAE
[3] Department of Aerospace Engineering/Department of Astronomy/NCSA CAPS, University of Illinois at Urbana-Champaign, Urbana, IL, USA
Received 2024 April 15; revised 2024 August 28; accepted 2024 August 28; published 2024 October 28

Abstract

In this work we revisit the problem of the dynamical stability of hierarchical triple systems with applications to circumbinary planetary orbits. We derive critical semimajor axes based on simulating and analyzing the dynamical behavior of 3×10^8 binary star–planet configurations. For the first time, three-dimensional and eccentric planetary orbits are considered. We explore systems with a variety of binary and planetary mass ratios, binary and planetary eccentricities from 0 to 0.9, and orbital mutual inclinations ranging from 0° to 180°. Planetary masses range between the size of Mercury and the lower fusion boundary (approximately 13 Jupiter masses). The stability of each system is monitored over 10^6 planetary orbital periods. We provide empirical expressions in the form of multidimensional, parameterized fits for two borders that separate dynamically stable, unstable, and mixed zones. In addition, we offer a machine learning model trained on our data set as an alternative tool for predicting the stability of circumbinary planets. Both the empirical fits and the machine learning model are tested for their predictive capabilities against randomly generated circumbinary systems with very good results. The empirical formulae are also applied to the Kepler and TESS circumbinary systems, confirming that many planets orbit their host stars close to the stability limit of those systems. Finally, we present a REST application programming interface with a web-based application for convenient access to our simulation data set.

Unified Astronomy Thesaurus concepts: Celestial mechanics (211)

Motivations for this work:

i) The above circumbinary stability criteria only cover parts of the parameter space.

ii) The various definitions of stability used in past works may result in misclassification of circumbinary planetary orbits as stable while they are actually unstable or vice versa.

Aims of this work:

i) To extend and homogenize the results of previous studies on the dynamical stability of circumbinary planetary orbits

ii) To remedy the limitations and inconsistencies that arise from combining stability estimates from different works by carrying out a self-consistent set of numerical simulations over long timescales.

Parameter Space:

Masses:

$$M_b = \frac{m_2}{m_1 + m_2} \text{ and } M_p = \frac{m_p}{m_1 + m_2}$$

$M_b \in \{0.5, 0.3, 0.1, 0.05, 0.02, 0.01\}$

$M_p \in \{10^{-2}, 10^{-3}, 10^{-4}, 10^{-5}, 10^{-6}, 10^{-7}\}$

Eccentricities: $e_b, e_p \in \{0, 0.1, 0.2, 0.3, 0.4, 0.5, 0.6, 0.7, 0.8, 0.9\}$

Mutual Inclination: $I_m \in \{0°, 18°, 36°, 54°, 72°, 90°, 108°, 126°, 144°, 162°, 180°\}$.

Planetary slowly varying angles: $\varpi_p, \omega_p, \Omega_p \in \{0^o, 90^o, 180^o\}$

Planetary true anomaly: $f_p \in \{0°, 45°, 90°, 135°, 180°, 225°, 270°, 315°\}$

Binary true anomaly: $f_b \in \{0^o, 180^o\}$

Integration time=1000000 planetary orbital periods Semi-major axis resolution=0.1

New Astronomy 23-24 (2013) 41–48

Contents lists available at SciVerse ScienceDirect

New Astronomy

journal homepage: www.elsevier.com/locate/newast

The dependence of the stability of hierarchical triple systems on the orbital inclination

Nikolaos Georgakarakos *

∈

Integration time=1000000 planetary orbital periods   Semi-major axis resolution=0.1

Criteria for instability

For any initial position of the planet:

i) either of the binary or planetary orbital eccentricity becomes ≥ 1
ii) orbit crossing
iii) $a_b \leq 0.001$ or $a_b \geq 100$
iv) $a_p \geq 1000$

Looking for two critical borders:

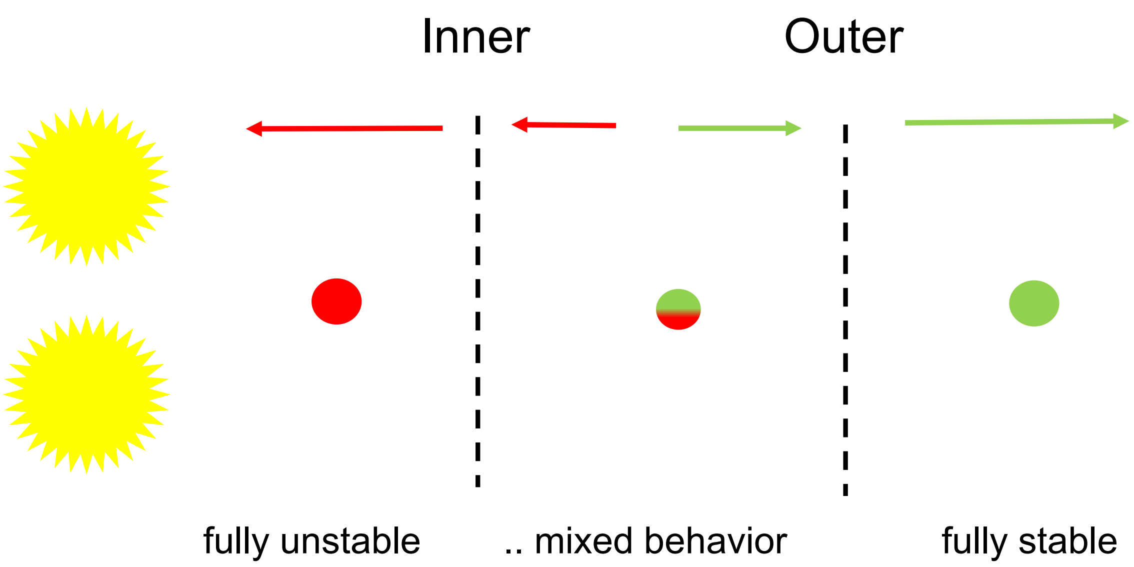

Parameters involved in our problem:

masses, eccentricities, semi-major axes, coplanarity of the system, various orbital angles

and

the integration time!

NYUAD HPC ~ 50000 cores

Results

Effect of each parameter on the stability borders:

- binary mass ratio: moderate effect
- planetary mass ratio: insignificant effect
- binary eccentricity: moderate effect
- planetary eccentricity: strongest effect
- mutual inclination: moderate effect
- planetary pericenter: small effect
- node: insignificant effect

Results

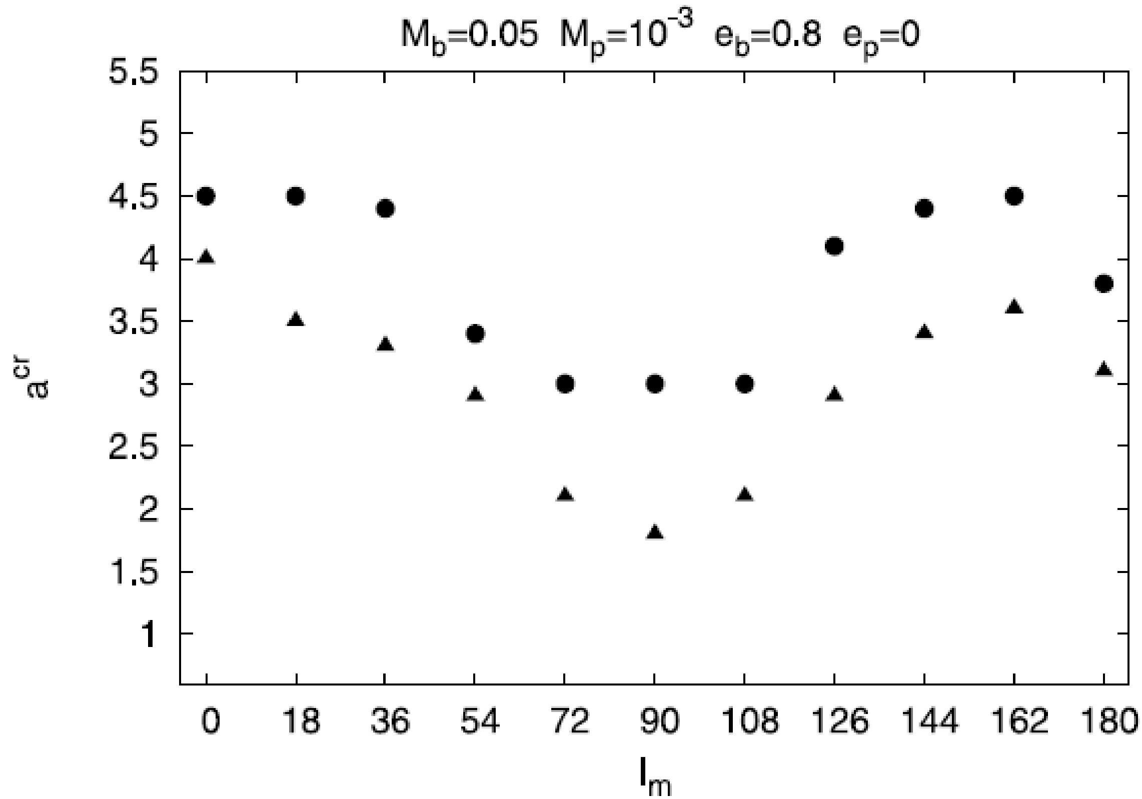

Figure 5. Critical semimajor axis against mutual inclination for a system with $M_b = 0.05$, $M_p = 10^{-3}$, $e_b = 0.8$, and $e_p = 0$. The triangles represent the inner critical border while the circles indicate the outer one.

In agreement with Doolin & Blundell (2011), Chen et al. (2020)

Georgakarakos et al. (2024)

Results

Effect of each parameter on the stability borders:

- binary mass ratio: moderate effect
- planetary mass ratio: insignificant effect
- binary eccentricity: moderate effect
- planetary eccentricity: strongest effect
- mutual inclination: moderate effect
- planetary pericenter: small effect
- node: insignificant effect

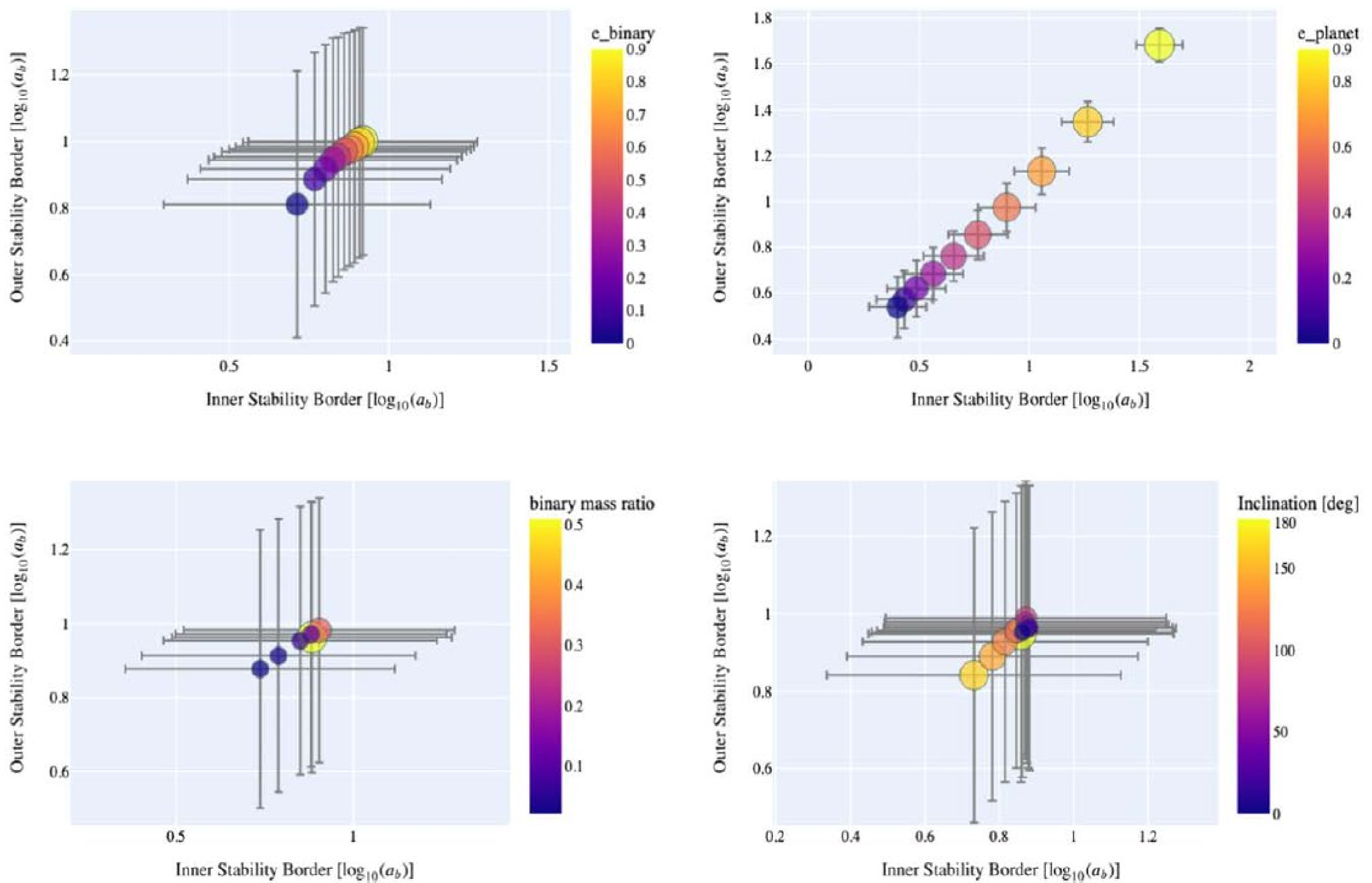

Figure 2. Mean and standard deviation of outer vs. inner stability borders in units of $\log_{10}$ of the binary semimajor axis. The color scale refers to the binary orbit eccentricity (top left), the planet's orbital eccentricity (top right), the binary mass ratio (bottom left), and the mutual inclination (bottom right). Stability limits depend strongly on the planetary orbital eccentricity, which accounts for most of the variance in the system. Stability borders also show roughly the same sensitivity to the orbital eccentricity of the binary star, the binary mass ratio, and the inclination of the system.

Georgakarakos et al. (2024)

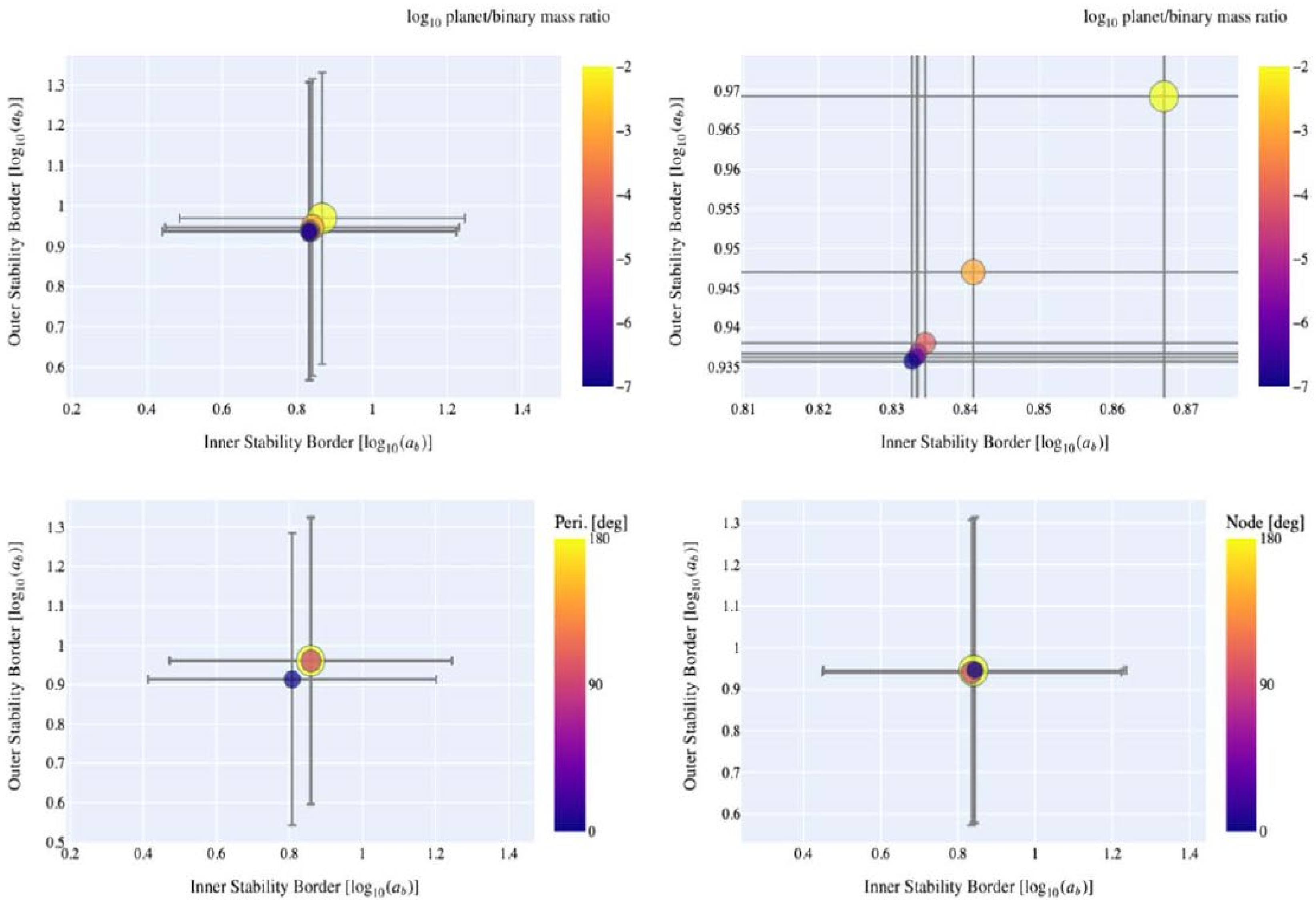

Figure 3. Same as Figure 2, but for the planet to binary mass ratio $M_p = m_p/(m_1 + m_2)$ (top left), a zoomed-in plot of the same (top right), the pericenter (bottom left), and the longitude of the ascending node (bottom right). In the parameter regime we have chosen for this study, the planet's mass does not substantially affect the stability limits. Aligned pericenters lead to lower instability in a system. The relative position of the nodes does not significantly impact the location of stability limits.

Georgakarakos et al. (2024)

Fitting formulae

- For every set of values (M_b, M_p, e_b, e_p, I_m), we had 9 critical distance values for different combinations of (Ω_p , ω_p). We retained the largest value for the outer critical border and the smallest value for the inner critical border (better markers for our borders – 2 variables down).

Fitting formulae

- For every set of values (M_b, M_p, e_b, e_p, I_m), we had 9 critical distance values for different combinations of (Ω_p , ω_p). We retained the largest value for the outer critical border and the smallest value for the inner critical border (better markers for our borders – 2 variables down).

- Planetary mass dropped.

Fitting formulae

- For every set of values (M_b, M_p, e_b, e_p, I_m), we had 9 critical distance values for different combinations of (Ω_p , ω_p). We retained the largest value for the outer critical border and the smallest value for the inner critical border (better markers for our borders – 2 variables down).

- Planetary mass dropped.

- Binary mass ratio and critical distances were rescaled using $\log_{10}$. Mutual inclination in radians.

Fitting formulae

- For every set of values (M_b, M_p, e_b, e_p, I_m), we had 9 critical distance values for different combinations of (Ω_p , ω_p). We retained the largest value for the outer critical border and the smallest value for the inner critical border (better markers for our borders – 2 variables down).

- Planetary mass dropped.

- Binary mass ratio and critical distances were rescaled using $\log_{10}$. Mutual inclination in radians.

- Third order polynomial fit selected. X^2 testing was used to control the quality of the fits.

Fitting formulae

- For every set of values (M_b, M_p, e_b, e_p, I_m), we had 9 critical distance values for different combinations of (Ω_p , ω_p). We retained the largest value for the outer critical border and the smallest value for the inner critical border (better markers for our borders – 2 variables down).

- Planetary mass dropped.

- Binary mass ratio and critical distances were rescaled using $\log_{10}$. Mutual inclination in radians.

- Third order polynomial fit selected. X^2 testing was used to control the quality of the fits.

- Two fits constructed: one for $e_p \leq 0.8$ and one for all e_p.

B coefficient vector, C uncertainties vector, X parameter vector

$$a_i^{cr} = a_b \times 10^{(B_i \pm C_i)\cdot X_i} \quad \text{and} \quad a_o^{cr} = a_b \times 10^{(B_o \pm C_o)\cdot X_o}$$

For $e_p \leq 0.8$

Inner border

$$\begin{aligned} B_i = (&0.20729,\ -0.32875,\ 0.10339,\ 0.58433,\ 0.36623,\\ &-0.25569,\ -0.06425,\ -0.38387,\ 1.01951,\ 0.26910,\\ &0.38912,\ -0.19863,\ -0.25361,\ -0.30333,\\ &0.09080,\ -0.05955),\end{aligned}$$

$$\begin{aligned} C_i = (&0.003763,\ 0.01015,\ 0.00224,\ 0.00922,\ 0.00978,\\ &0.00982,\ 0.00069,\ 0.00947,\ 0.01176,\ 0.00687,\\ &0.00759,\ 0.00420,\ 0.00735,\ 0.00913,\\ &0.00129,\ 0.00280),\end{aligned}$$

$$\begin{aligned} X_i = (&1,\ M_{lb},\ I_m,\ e_b,\ e_p,\ M_{lb}^2,\ I_m^2,\ e_b^2,\ e_p^2,\ M_{lb}e_b,\\ &M_{lb}e_p,\ I_m e_b,\ M_{lb}e_b^2,\ M_{lb}e_p^2,\ I_m^2 e_b,\ M_{lb}^3).\end{aligned}$$

Outer border

$$\begin{aligned} B_o = (&0.23612,\ -0.29377,\ 0.22710,\ 1.06753,\ 0.62109,\\ &-0.21512,\ -0.06648,\ -1.52936,\ -0.4748,\ -0.31329\\ &-0.00869,\ 0.11846,\ -0.03932,\ -0.00933,\\ &0.87506,\ 1.25895),\end{aligned}$$

$$\begin{aligned} C_o = (&0.00317,\ 0.00927,\ 0.00313,\ 0.00905,\ 0.00975,\\ &0.00910,\ 0.00202,\ 0.02330,\ 0.02893,\ 0.00389,\\ &0.00116,\ 0.00119,\ 0.00260,\ 0.00041,\\ &0.01699,\ 0.02373),\end{aligned}$$

$$\begin{aligned} X_o = (&1,\ M_{lb},\ I_m,\ e_b,\ e_p,\ M_{lb}^2,\ I_m^2,\ e_b^2,\ e_p^2,\ I_m e_b,\ I_m e_p,\ I_m^2 e_b,\\ &M_{lb}^3,\ I_m^3,\ e_b^3,\ e_p^3).\end{aligned}$$

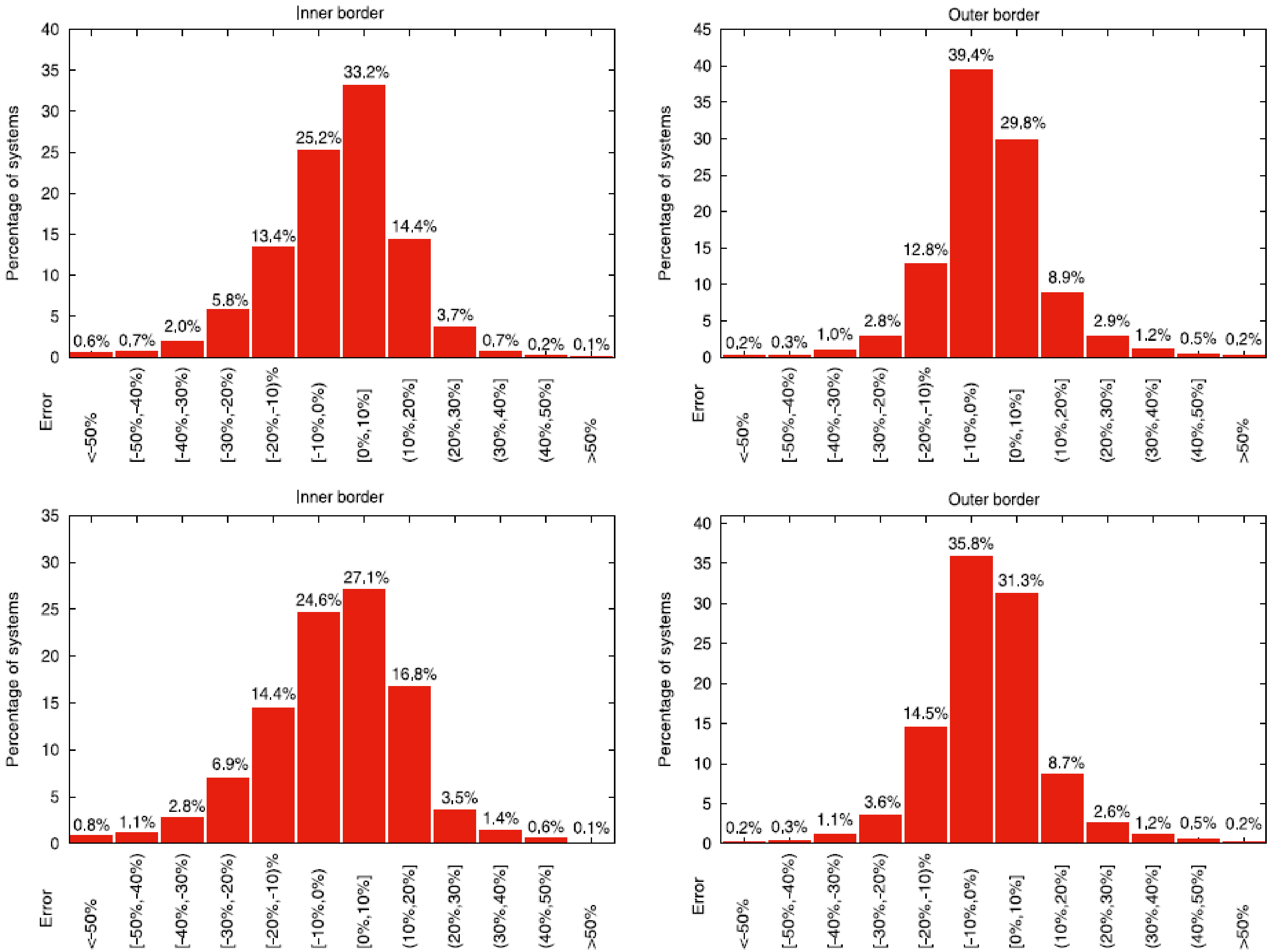

Figure 8. Relative percentage error distribution from comparing our empirical fits against the results of numerical simulations. On the x-axis we have bins of relative percentage error between the results from the numerical simulations and the fits of Equations (10), while on the y-axis we have the percentage of systems that fall into a specific error bin. The top row is for the $e_P \leqslant 0.8$ case, while the bottom row plots represent the more eccentric case.

Georgakarakos et al. (2024)

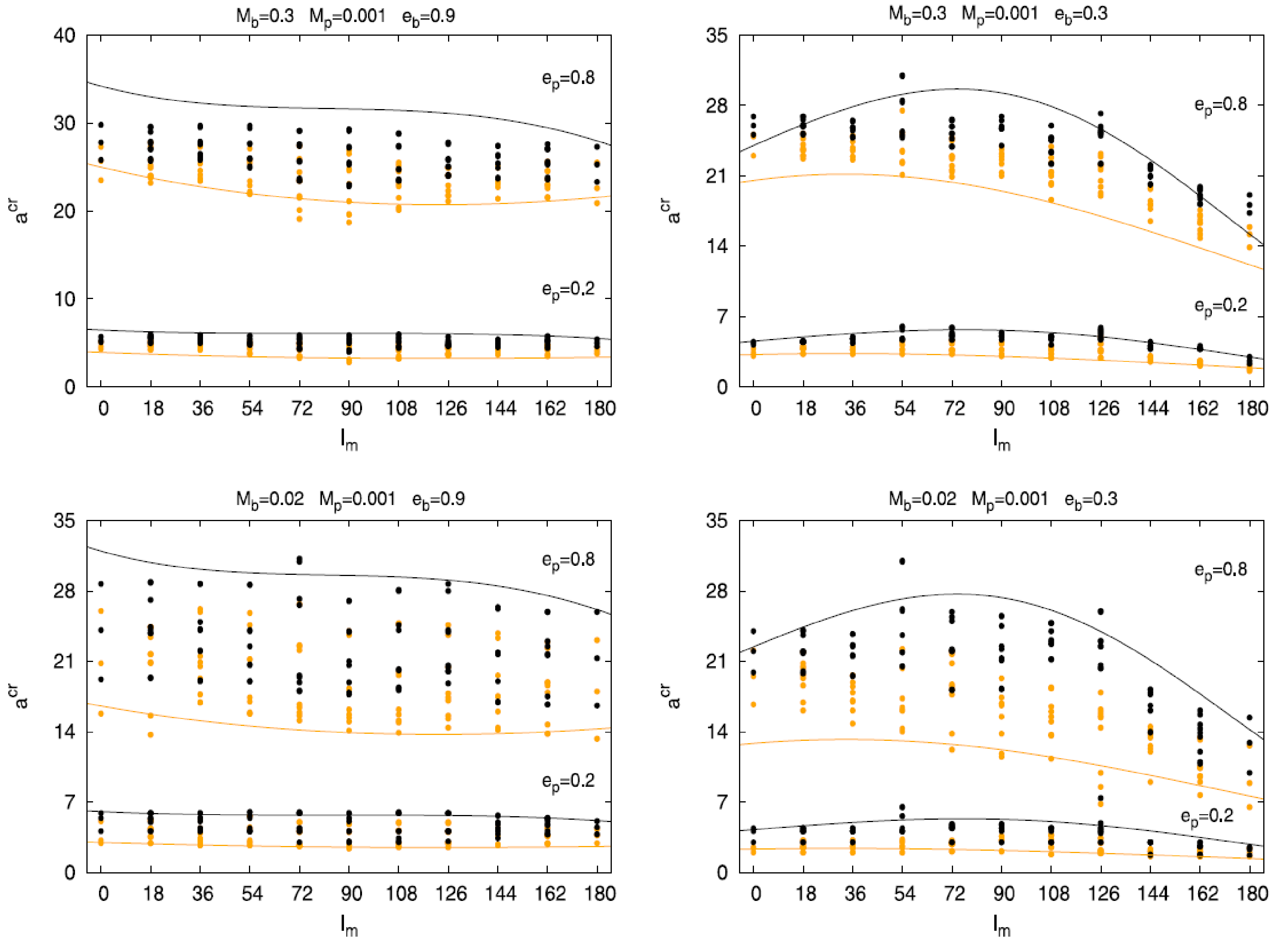

Figure 9. Critical semimajor axis against mutual inclination for a variety of systems. The orange color refers to the inner boundary, while the black color denotes the outer stability border. The continuous lines are our empirical fits as given in Section 3.2. The points are the output from the numerical simulations for the specific systems. Note that the majority of the points lie between the two curves, as they ideally should.

Georgakarakos et al. (2024)

Fit performance against random simulations

In order to test the quality of our fitting formulae, we carried out a number of additional, randomly generated, simulations. We drew parameter values for our random systems from a uniform distribution within the ranges used for the creation of the simulation dataset. The planetary semi-major axis was sampled using rejection sampling upon distributions created from our simulation dataset.

50000 systems were created in total.

Classification of the Results of Random Simulations Using the Fits Given in Section 3.2

Inner Border Distribution				
N.U.I.P.	Stable	Quantity per Zone Mixed	Unstable	Total
0	**12,148 (54.7%)**	**1826 (8.2%)**	1 (0.0%)	13,975 (62.9%)
1–15	216 (1.0%)	**1825 (8.2%)**	32 (0.1%)	2073 (9.3%)
16	54 (0.2%)	**2245 (10.1%)**	**3877 (17.5%)**	6176 (27.8%)
Total	12,418 (55.9%)	5896 (26.5%)	3910 (17.6%)	22,224 (100.0%)

Outer Border Distribution				
N.U.I.P.	Stable	Quantity per Zone Mixed	Unstable	Total
0	**14,905 (66.8%)**	**1712 (7.7%)**	2 (0.0%)	16,619 (74.5%)
1–15	177 (0.8%)	**1468 (6.5%)**	18 (0.1%)	1663 (7.4%)
16	37 (0.2%)	**1685 (7.5%)**	**2320 (10.4%)**	4042 (18.1%)
Total	15119 (67.8%)	4865(21.8%)	2340 (10.5%)	22324 (100.0%)

Notes. N.U.I.P: number of unstable initial positions of the planet on its initial orbit. The percentages refer to the number of individual cases over the total number of cases. For the interpretation of numbers in bold please see the main body of the paper.

Success rates:

Inner = 80.4% - 98.7%

Success rates:

Outer = 83.7% - 98.9%

Application to known circumbinary systems

Parameter Values of Circumbinary Systems Used for the Validation of the Empirical Stability Fits

System	m_1 ($M_\odot$)	m_2 ($M_\odot$)	m_p (M_J)	I_m (deg)	a_b (au)	a_p (au)	e_b	e_p
Kepler-16	0.6897	0.20255	0.333	0.4	0.22431	0.7048	0.15944	0.00685
Kepler-34	1.0479	1.0208	0.22	1.81	0.22882	1.0896	0.52087	0.182
Kepler-35	0.8876	0.8094	0.127	1.28	0.17617	0.60345	0.1421	0.042
Kepler-38	0.949	0.249	0.384	0.182	0.1469	0.4646	0.1032	0.032
Kepler-47 b	0.957	0.342	0.006513	0.166	0.08145	0.2877	0.0288	0.021
Kepler-47 c	0.957	0.342	0.05984	1.165	0.08145	0.6992	0.0288	0.024
Kepler-47 d	0.957	0.342	0.00997	1.38	0.08145	0.9638	0.0288	0.044
Kepler-64	1.528	0.378	0.531	2.814	0.1744	0.634	0.2117	0.0539
Kepler-413	0.82	0.5423	0.21	4.073	0.10148	0.3553	0.0365	0.1181
Kepler-453	0.944	0.1951	0.05	2.258	0.18539	0.7903	0.0524	0.0359
Kepler-1647	1.21	0.975	1.52	2.9855	0.1276	2.7205	0.1593	0.0581
Kepler-1661	0.841	0.262	0.053	0.93	0.187	0.633	0.112	0.057
TIC 172900988	1.2388	1.2023	2.74	1.45	0.191928	0.89809	0.44793	0.088
TOI-1338 b	1.127	0.3313	0.0685	0	0.1321	0.4607	0.155522	0.088
TOI-1338 c	1.127	0.3313	0.205	0-180	0.1321	0.794	0.155522	0.16

Stability Borders for Known Circumbinary Systems

System	a_i^{cr} (au)	a_o^{cr} (au)	a_p (au)
Kepler-16	0.551	0.688	0.705
Kepler-34	0.804	1.092	1.090
Kepler-35	0.410	0.511	0.603
Kepler-38	0.349	0.427	0.464
Kepler-47 b	0.178	0.198	0.288
Kepler-47 c	0.179	0.200	0.699
Kepler-47 d	0.181	0.206	0.964
Kepler-64	0.457	0.627	0.634
Kepler-413	0.236	0.281	0.355
Kepler-453	0.427	0.504	0.790
Kepler-1647	0.310	0.397	2.720
Kepler-1661	0.452	0.570	0.633
TIC 172900988	0.579	0.784	0.898
TOI-1338 b	0.337	0.448	0.461
TOI-1338 c	0.361	0.492	0.794

Table 3. Critical planetary semimajor axis for Kepler-16, Kepler-34, Kepler-35, Kepler-38, Kepler-64 and Kepler 413. 'W', 'O', 'K13', 'S' and 'K14' stand for Welsh et al. (2012), Orosz et al. (2012b), Kostov et al. (2013), Schwamb et al. (2013) and Kostov et al. (2014), respectively.

System	Nominal (au)	Numerical (au)	Holman & Wiegert (au)	Mardling & Aarseth (au)	Published (au)
Kepler-16	0.7048	0.67	0.65	0.64	0.59 (W)
Kepler-34	1.0896	1.00	0.84	0.87	0.88 (W)
Kepler-35	0.603 45	0.52	0.50	0.53	0.49 (W)
Kepler-38	0.4644	0.43	0.39	0.43	0.37 (O)
Kepler-64 (K13)	0.642	0.65	0.53	0.58	– (K13)
Kepler-64 (S)	0.634	0.58	0.52	0.53	0.57 (S)
Kepler-413	0.3553	0.31	0.26	0.35	– (K14)

Chavez et al. (2015)

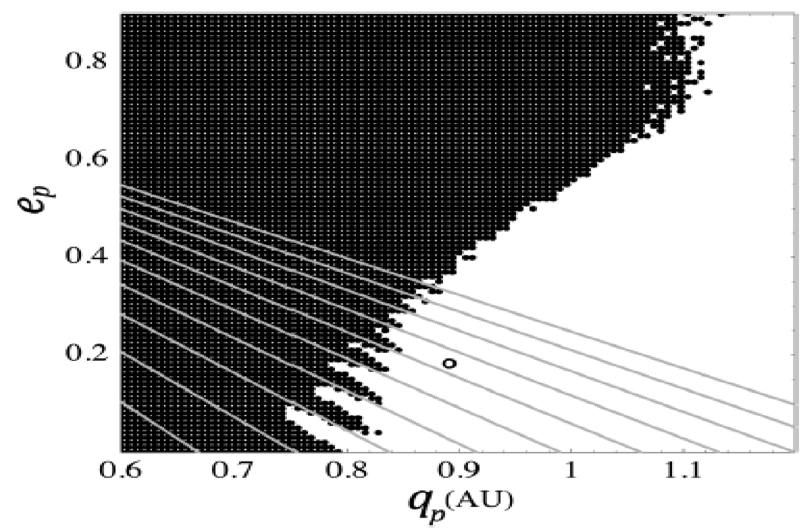

Figure 3. Eccentricity e_p against pericentre distance q_p for Kepler-34b. The integration time is 10^5 yr. The open circle is the nominal position of the planet, and the light-grey lines correspond to the locations of certain mean motion resonances between the stellar and planetary orbits. From left to right the resonances shown here are: 5:1, 6:1, 7:1, 8:1, 9:1, 10:1, 11:1, 12:1, 13:1 and 14:1.

Comparison with other results

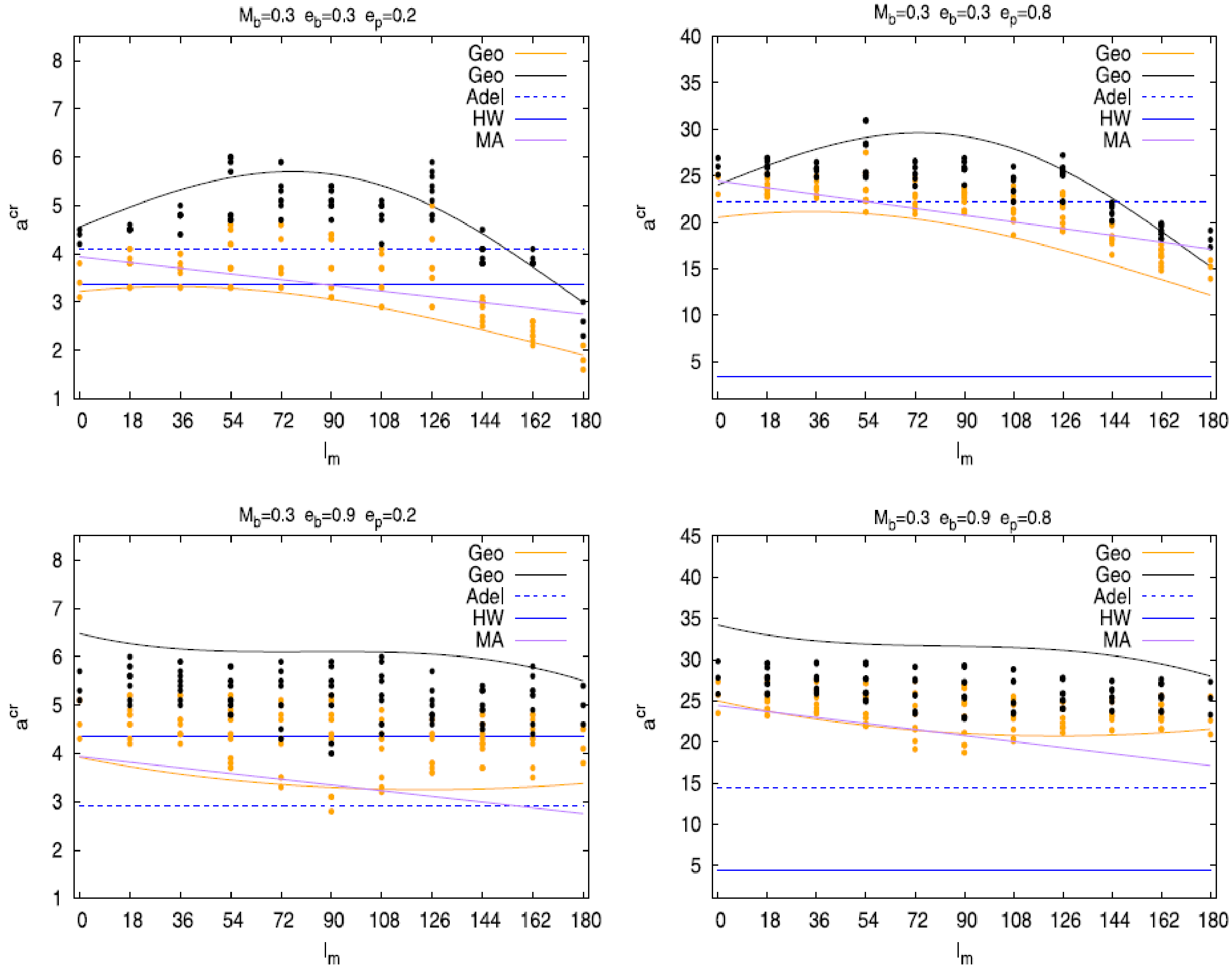

Figure 11. Comparison between different stability fits. Geo stands for the fits of the present work, Adel denotes the work by S. Adelbert et al. (2023), HW denotes the classification formula given in M. J. Holman & P. A. Wiegert (1999), and MA stands for the criterion developed by R. Mardling & S. Aarseth (1999) and R. A. Mardling & S. J. Aarseth (2001). As previously, the black color denotes the outer critical border, while the orange color represents the inner critical border. The circles are the results from our numerical simulations.

Georgakarakos et al. (2024)

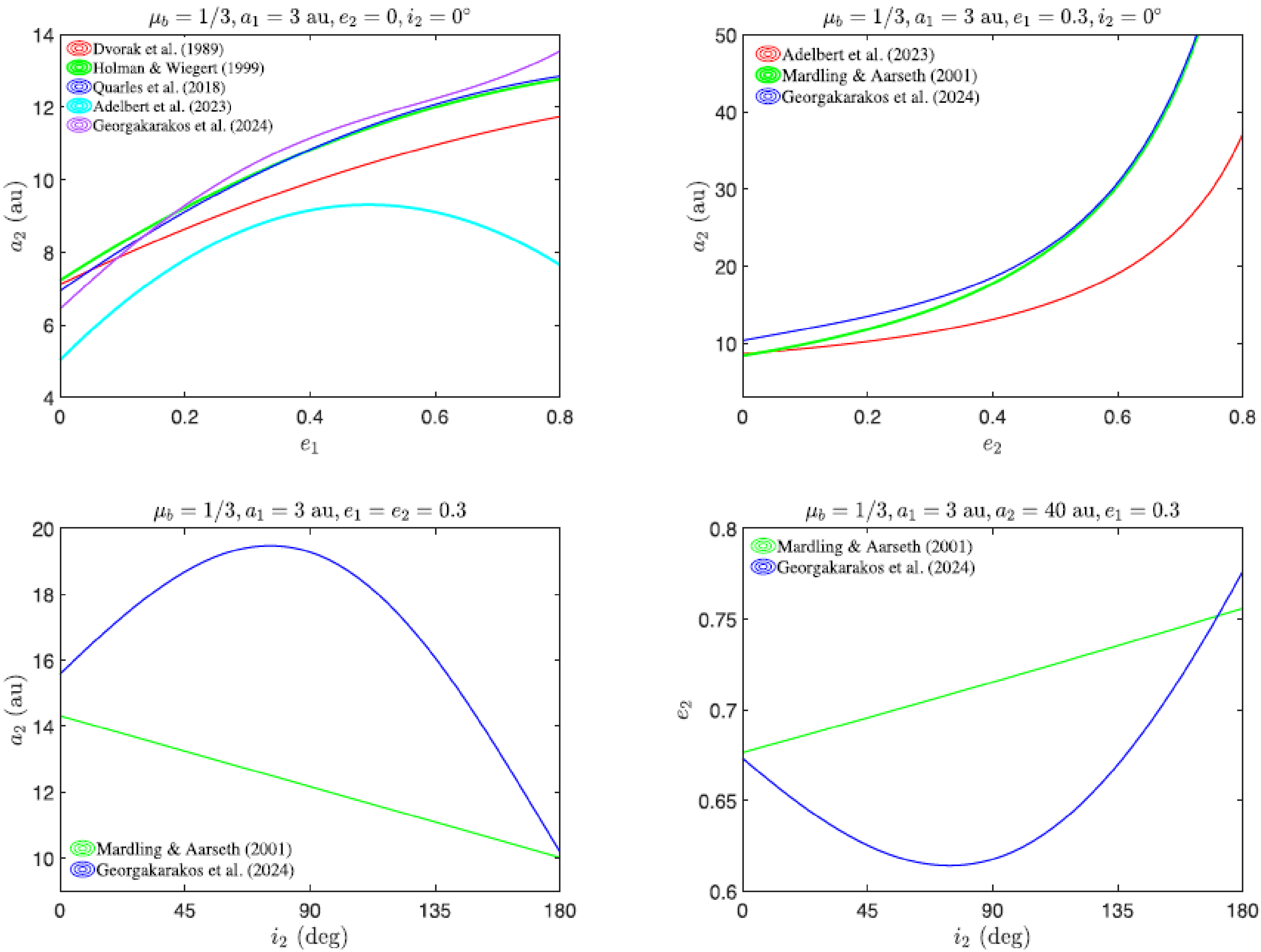

Lei & Gong (2024)

We have also trained a Machine Learning model with our simulation data (XGBRegressor model – Chen & Guestrin 2016).

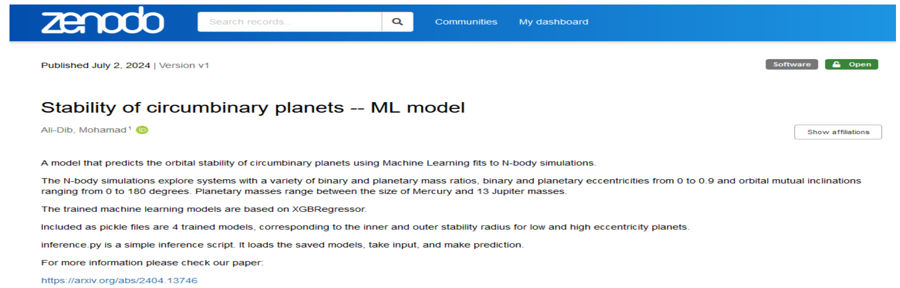

Classification of the Results of Random Simulation Using the Machine Learning Model ($e_p \leqslant 0.8$)

Inner Border Distribution				
N.U.I.P.	Stable	Quantity per Zone Mixed	Unstable	Total
0	**12,658 (57.0%)**	**1312** (5.9%)	5 (0.0%)	13,975 (62.9%)
1–15	382 (1.7%)	**1671** (7.5%)	20 (0.1%)	2073 (9.3%)
16	133 (0.6%)	**2560** (11.5%)	**3483 (15.7%)**	6176 (27.8%)
Total	13,173 (59.3%)	5543 (24.9%)	3508 (15.8%)	22,224 (100.0%)
Outer Border Distribution				
N.U.I.P.	Stable	Quantity per Zone Mixed	Unstable	Total
0	**15,415 (69.1%)**	**1203** (5.4%)	1 (0.0%)	16,619 (74.5%)
1–15	300 (1.3%)	**1344** (6.0%)	19 (0.1%)	1663 (7.4%)
16	99 (0.5%)	**1884** (8.4%)	**2059** (9.2%)	4042 (18.1%)
Total	15,814 (70.9%)	4431 (19.8%)	2079 (9.3%)	22,324 (100.0%)

The ML model was tested against the 50000 randomly chosen systems with very good results.

Online portal and Application Programmng Interface (API)

A software interface designed to facilitate interaction with large catalogs of numerical stability simulations such as constructed in this Work.

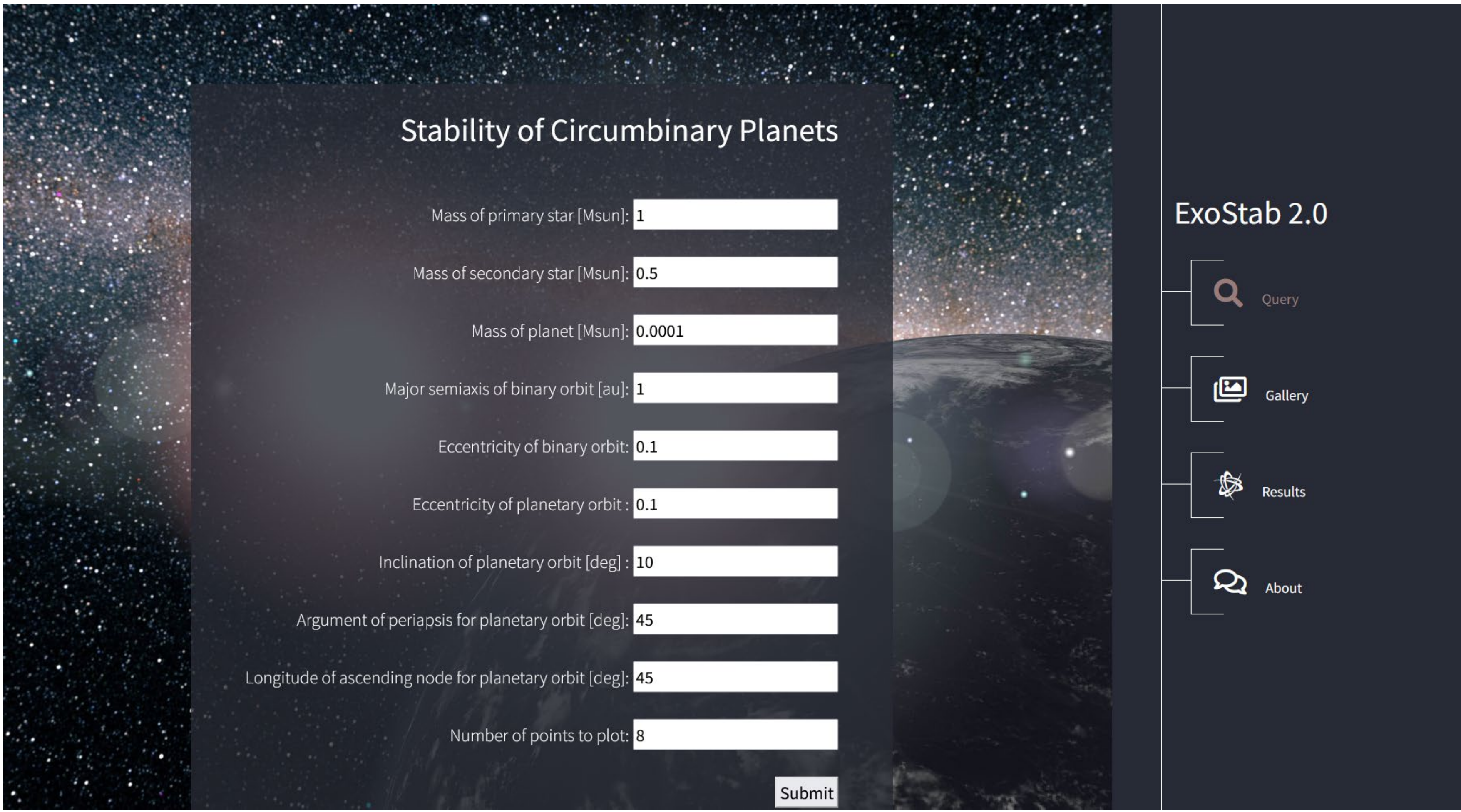

Summary

- We investigated the dynamical stability of circumbinary planets by carrying out a very large number of numerical simulations covering almost completely the parameter space

- We derived empirical formulae for the critical planetary distances

- We trained a Machine Learning model as an additional predictive tool

- We tested our tools against real and synthetic systems, as well as against older stability formulae with excellent results.

- We provide an online portal and application programming interface for accessing our simulation dataset.

- **More information can be found in Georgakarakos et al. (2024), AJ, 168, id.224.**